*Korean J. Chem. Eng.*, 32(3), 478-485 (2015)
DOI: 10.1007/s11814-014-0249-2

pISSN: 0256-1115
eISSN: 1975-7220

# Removal of strontium ions from nuclear waste using synthesized $MnO_2$-$ZrO_2$ nano-composite by hydrothermal method in supercritical condition

**Seyed Javad Ahmadi*,†, Neda Akbari*, Zahra Shiri-Yekta*, Mohammad Hossein Mashhadizadeh**, and Morteza Hosseinpour***

*Nuclear Science and Technology Research Institute, P. O. Box 11365/8486, Tehran, Iran
**Faculty of Chemistry, Tarbiat Moallem University, Tehran, Iran
(*Received 14 January 2014 • accepted 26 August 2014*)

**Abstract**−This study focuses mainly on the synthesis of $MnO_2$-$ZrO_2$ nano-composite as a new inorganic adsorbent. Supercritical water was used as a preparation medium for particle deposited materials. $MnO_2$-$ZrO_2$ was prepared from metal nitrate solutions in supercritical region. The resulting sample was characterized by Fourier transform infrared (FTIR), X-ray fluorescence (XRF), X-ray powder diffraction (XRD), thermogravimetric analysis (TGA) and transmission electron microscope (TEM). Analyses of the TEM images show the possibility for crystallizing nano-sized particles. The synthesized adsorbent was then used for the removal of strontium(II) from the nuclear waste. Moreover, a number of factors such as aqueous phase pH, contact time and initial metal ions concentration in the adsorption process were investigated. Comparison of the adsorption efficiency of the $MnO_2$-$ZrO_2$ nano-particles with those of the non-nano particles shows a shift of uptake of the metal ions vs. pH curves towards lower pH values and a significant improvement in adsorption of strontium ions was observed by using the nano-adsorbent. The kinetic data corresponds well to the pseudo-second-order equation. The adsorption data for strontium(II) were well fitted by the Langmuir isotherm. The synthesized nano-composite also showed a strong affinity toward the removal of Y(III), Ni(II), Pb(II) and Co(II) from the nuclear radioactive waste.

Keywords: Supercritical Water Synthesis, $MnO_2$-$ZrO_2$ Nano-composite, Ion Exchanger, Strontium, Adsorption

## INTRODUCTION

The removal of toxic heavy metal pollutants from industrial wastewaters has become a considerable problem for developing industrial activities. Radiostrontium, when accumulated in human bones, is considered one of the most hazardous pollutants because of the chemical and biochemical similarities with calcium. Therefore, methods of processing of strontium-containing wastewaters have attracted much attention of technologists.

There have been many different methods for treating wastewater, including precipitation, liquid-liquid extraction, sedimentation, flotation, filtration, membrane processes, electrochemical techniques, biological process, chemical reactions, adsorption and ion exchange. However, selection of the wastewater treatment method is based on the concentration of waste and the cost of treatment. From the point of view of sorption processes, numerous inorganic materials demonstrate proven ability to effectively remove the heavy metals from wastewaters [1,2].

During the past decade, intensive work has been done on nanostructured inorganic materials because of their unusual physical and chemical properties owing to their extremely small size and large specific surface area [3]. Thus, nanomaterials have found wide applications in the adsorption and removal of heavy metal ions from industrial wastewater [4-7]. To follow this interesting procedure, there is an incentive to develop a novel adsorbent with a large surface area for adsorption, a small diffusion resistance, and a high capacity for large solutes.

Supercritical water has been the subject of a wide variety of researches, largely due to its enhanced properties (high density, high diffusivity, low viscosity, etc.), as well as the ability to control its properties by varying the pressure and temperature conditions. One application that has been a focus of some researchers is hydrothermal synthesis reaction in supercritical water. This method, which was employed by Adschiri and co-workers as a means of producing fine metal oxide particles [8-16], is used in the production of metal oxide crystals from metal aqueous salt solutions by heating the solution. This reaction is represented by the following two steps, hydrolysis and dehydration.

$$M(NO_3)_x+xH_2O=M(OH)_x+xHNO_3 \text{ (hydrolysis)} \quad (i)$$

$$M(OH)_x=MO_{x/2}+x/2H_2O \text{ (dehydration)} \quad (ii)$$

It has been reported that in the supercritical region, fast reaction rates and low metal oxide solubility lead to an extremely high nucleation rate, which also allows the formation of nano-sized particles.

In the present work, the $MnO_2$-$ZrO_2$ nano-composite was synthesized by using supercritical method. The size, structure and properties of $MnO_2$-$ZrO_2$ were investigated and were applied for removal of strontium ions from the nuclear waste. The results were compared with amorphous $MnO_2$-$ZrO_2$ composite [17]. This nanocomposite showed high ion-exchange ability towards strontium ions in comparison with $MnO_2$-$ZrO_2$ non-nano adsorbent. In fact,

†To whom correspondence should be addressed.
E-mail: sjahmadi@aeoi.org.ir, sjahmadi@yahoo.com

a shift of the uptake percentage towards lower pH values, and considerable augmentation of removal of strontium ions have resulted by replacing amorphous $MnO_2$-$ZrO_2$ composite by the nano-adsorbent. Then, the parameters affecting adsorption properties were investigated and discussed.

The adsorption efficiency of the studied adsorbent for strontium ion was compared with some other adsorbents reported in the literature. For example, Moon et al. studied PAN/$K_2Ti_4O_9$ as a sorption material whose $K_d$ value for adsorption of strontium ions was equal to 940 mL/g [18]. The sorption behavior of potassium hexacyanocobalt (II) ferrate (II) (KCFC) was studied for strontium ion and reported 10,760 mL/g for the adsorption efficiency [19]. Ion-exchangers, stannic molybdophosphate (SMP) and stannic molybdophosphate in the polyacrylamide (SMP-PAA) showed $K_d$ values for the adsorption of strontium ions equal to >5,000 and >10,000 mL/g, respectively [20]. Potassium zinc hexacyanoferrate(II) (PZF) sorbent provided $K_d$ equal to ~2,300 mL/g for strontium ion [21]. Therefore, according to the results obtained here ($K_d$~30,000 mL/g), the main advantage of the sorbent used is its significant improvement in the uptake of strontium ions.

## EXPERIMENTAL

### 1. Materials and Reagents

Manganese(II) nitrate, zirconium(IV) oxide chloride and potassium hydroxide were purchased from Merck and were used as the starting materials without further purification. A stock solution of strontium was prepared by dissolving $Sr(NO_3)_2$ in deionized water. Amorphous $MnO_2$-$ZrO_2$ composite was prepared according to a reported procedure [17], in size (100 μm). All other reagents and chemicals were of analytical reagent grade.

### 2. Preparation of Adsorbent

The $MnO_2$-$ZrO_2$ nano-composite was synthesized according to a reported procedure [22]. The experiments were performed using a batch-type reactor which was heated until the system reached supercritical conditions of water (25-30 MPa and 380-450 °C) (Fig. 1). Aqueous solutions of $Mn(NO_3)_2$ and $ZrOCl_2$ solutions were loaded into the reactor at 450 °C during 1 h under varying conditions as given in Table 1. The effects of operational conditions on the yield, purity, and size of the metal oxide nano-particles were investigated in our previous study [23]. Accordingly, $MnO_2$-$ZrO_2$ nano-particles were made at optimized condition. Then, they were removed from the furnace and quenched by cold water. The produced $MnO_2$-$ZrO_2$ particles underwent numerous washing processes by distilled water with high-speed centrifuge procedure. Finally, they were spread on some Petri dishes and dried at ambient condition.

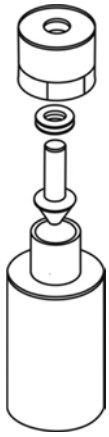

**Fig. 1. A schema of high pressure autoclave applied for synthesis of $MnO_2$-$ZrO_2$ nano-particles.**

### 3. Characterization of $MnO_2$-$ZrO_2$ Nano-composite

Powder X-ray diffraction (XRD, 3710 PW Philips) patterns of the adsorbent were measured by Cu-K$\alpha$ radiation. The X-ray source was a rotating anode operating at 40 kV and 30 mA with a copper target, and the data were collected between $2\theta$ of 20 and 80°. The amounts of manganese and zirconium were also determined by the X-ray fluorescence (XRF, Oxford ED2000). The morphology of the product was studied by transmission electron microscopy (TEM, LEO 912AB). Fourier transform infrared (FT-IR, Bruker Vector 22) spectrum was recorded using KBr disks. Thermogravimetry (TG) was carried out with a Rheometric Scientific 1500 at a heating rate of 10 °C/min.

### 4. Batch Studies

The ion-exchange capacity of hydrous $MnO_2$-$ZrO_2$ nano-composite for $K^+$ in aqueous solutions was determined by batch equilibration of 0.1 g of solid and 10 ml of 0.05 M of the KCl solution in a shaker water bath adjusted at 25±1 °C until equilibration was achieved [24-26]. After equilibration the phases were separated and analyzed. The adsorbent capacity (meq/g) and uptake percentage were calculated by Eqs. (1) and (2):

$$\text{Capacity} = C_0 \cdot Z \cdot \frac{\%Up}{100} \times \frac{V}{m} \quad (1)$$

$$Up = \frac{(C_0 - C_e)}{C_0} \times 100 \quad (2)$$

where $C_0$ and $C_e$ are the initial and equilibrium concentration of

**Table 1. Conditions of preparation $MnO_2$-$ZrO_2$ nano composite**

| Sample | Concentration of reagents[a] (M) | Mixing volume ratio, Mn : Zr | XRF analysis of nano composite | |
|---|---|---|---|---|
| | | | Percentage of Mn | Percentage of Zr |
| $MnO_2$-$ZrO_2$-1 | 0.5 | 1 : 1 | 9.8 | 71.0 |
| $MnO_2$-$ZrO_2$-2 | 0.5 | 1.5 : 1 | 18.8 | 62.3 |
| $MnO_2$-$ZrO_2$-3 | 0.5 | 3 : 1 | 54.3 | 21.6 |
| $MnO_2$-$ZrO_2$-4 | 0.5 | 5 : 1 | 47.5 | 41.4 |

[a]Solutions of $Mn(NO_3)_2$ and $ZrOCl_2$

ions (mg/*l*), respectively, V (ml) is the volume of the aqueous phase, m (g) is the mass of the adsorbent and Z is the charge of the metal ion adsorbed.

The distribution coefficient ($K_d$) gives an indication of the composite selectivity as well as of the maximum processing capacity of the studied cations. The values of $K_d$ were determined in batch experiments. Aliquot portions of strontium were placed in 20 mL polypropylene bottles after the adjustment of pH (by Schott, model CG841) to the desired value with dilute sodium hydroxide or hydrochloric acid. $MnO_2$-$ZrO_2$ nano-adsorbent (0.05 g) was added to 5 ml of 50 mg/L of metal ion solution, and the sample bottles were then placed in a thermostated shaker (Infors AG, Aquatron) at 25±1 °C. The concentration of the solution before and after equilibration was measured by inductively coupled plasma-atomic emission spectroscopy (ICP-AES, model Turbo AX 150 Liberty). The distribution coefficient values were calculated according to:

$$K_d = \frac{(C_0 - C_e)}{C_e} \times \frac{V}{m} \quad (3)$$

## RESULTS AND DISCUSSION

### 1. Physicochemical Characterization

The amounts of manganese and zirconium elements were determined using XRF spectroscopy in the synthesized composites according to the given conditions in Table 1. The obtained results showed that by increasing $Mn(NO_3)_2$ concentration in reaction to ratio 5 : 1 (Mn/Zr), the percentage of $MnO_2$ and $ZrO_2$ is approximately equal in the structure of $MnO_2$-$ZrO_2$ composite (See Table 1). Therefore, this sample for the next analysis was used. The thermal analysis data related to hydrous $MnO_2$-$ZrO_2$ nano-composite are given in Fig. 2. Thermogravimetric analysis of the ion exchanger showed a total weight loss of 66% at 800 °C. From the DSC curve, the observed endothermic peak at 80 °C was due to the removal of external water [27]. Also, the complete evaporation of water from the adsorbent structure has occurred at 378 °C and the hydrous $MnO_2$-$ZrO_2$ has converted to anhydrous oxide.

An FTIR spectrum in Fig. 3 shows a broad band centered on 3,500-3,000 $cm^{-1}$ which indicates the presence of hydroxyl groups. The peaks at 1,100-1,000 $cm^{-1}$ correspond to the bending vibration of water molecules, and the bands in the 800-500 $cm^{-1}$ region are due to the Mn-O and Zr-O stretching. It can be seen from TEM image (Fig. 4) that the composite sample consists of the nano-particles with sizes less than 30 nm on average. The X-ray powder diffraction patterns for the obtained $MnO_2$-$ZrO_2$ nano-composite were determined. The results were compared with X-ray related to $MnO_2$-$ZrO_2$ composite, which indicated that $MnO_2$-$ZrO_2$ had a crystalline structure (Fig. 5). Fig. 5 shows the XRD patterns of the $MnO_2$-$ZrO_2$ nano-composite that were compared with the standard XRD of $MnO_2$ ($2\theta$=32.91, 35.65 and 55.21), $ZrO_2$ ($2\theta$=29.65, 34.61, 49.61 and 59.25) and $MnZrO_2$ ($2\theta$=30.43, 35.26 and 50.78). The result indicates that the product has a crystalline structure and a combination of $MnO_2$ and $ZrO_2$.

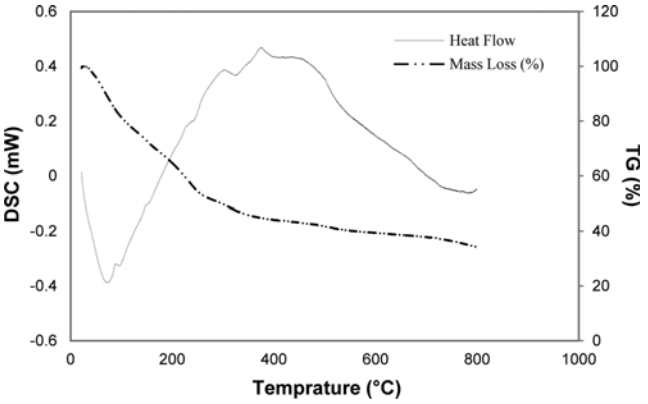


**Fig. 2. TGA and DSC curves for $MnO_2$-$ZrO_2$ nano-particles.**

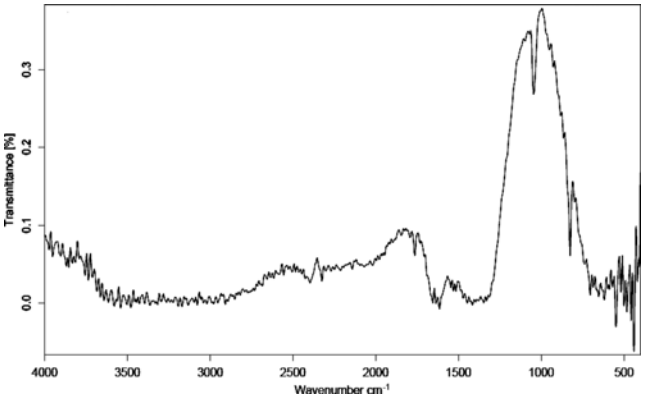


**Fig. 3. IR spectra of $MnO_2$-$ZrO_2$ nano-particles.**

Measurement of capacity of the $MnO_2$-$ZrO_2$ nano-composite and amorphous $MnO_2$-$ZrO_2$ composite for $K^+$ ion in aqueous solutions based on Eq. (1) showed that the ion-exchangers capacities were 2.9 and 1.5 meq/g, respectively. Therefore, $MnO_2$-$ZrO_2$ nano-

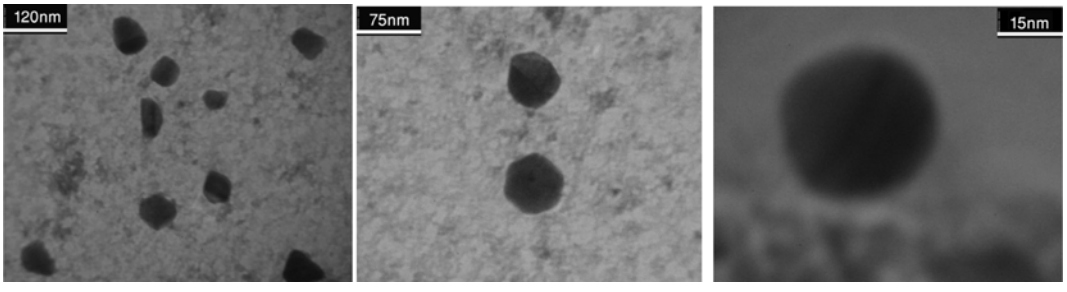


**Fig. 4. The TEM images of $MnO_2$-$ZrO_2$ prepared at 450 °C.**

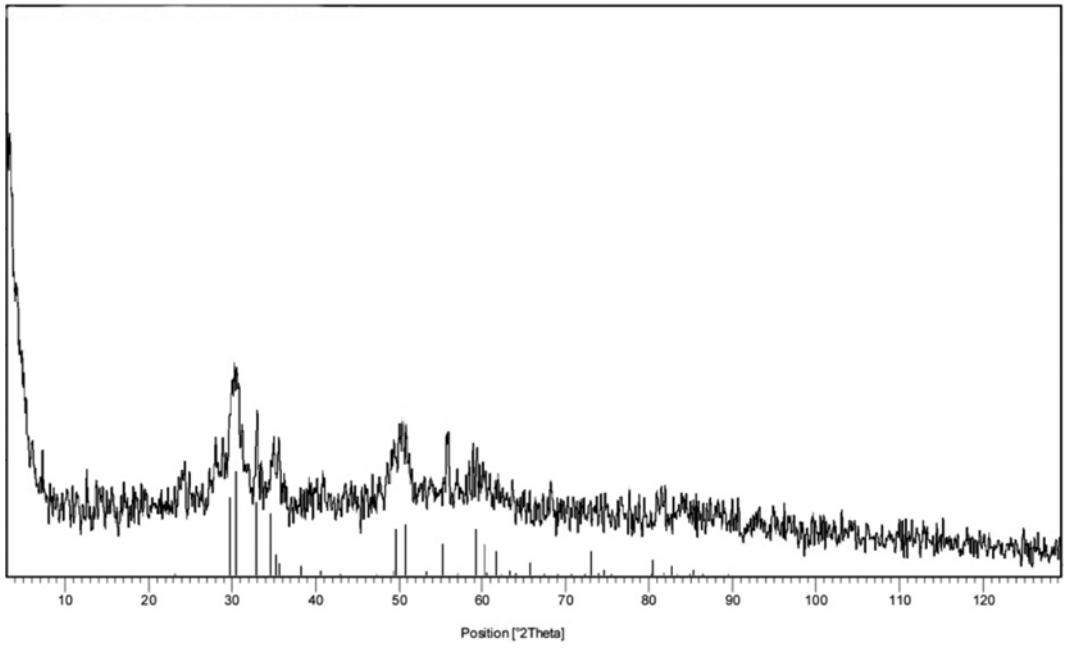


**Fig. 5. XRD patterns of $MnO_2$-$ZrO_2$ nano-particles prepared under supercritical conditions.**

composite with high ionic exchange capacity can be used for adsorption of strontium ions from aqueous phase.

**2. Effect of pH of Sample Solution**

The pH dependence of metal ion adsorption is a complex phenomenon which strongly influences the ion adsorption. To evaluate the effect of pH on the adsorption, competitive adsorption of Sr(II) ions (initial concentration 50 mg/*l*) on $MnO_2$-$ZrO_2$ nano-composite and amorphous $MnO_2$-$ZrO_2$ composite was studied at different pH values in the range 2-6. The results show the pH dependency of the adsorption process with both types of adsorbents (Fig. 6), which is a general phenomenon for most inorganic ion-exchangers from the group of transition metal oxides. With a lower pH, the oxide surface will have positive character and less affinity for Sr(II); on the other hand, with a higher pH, the oxide will behave as negatively charged surface, as a result of which the uptake is a maximum in basic solutions [28-30].

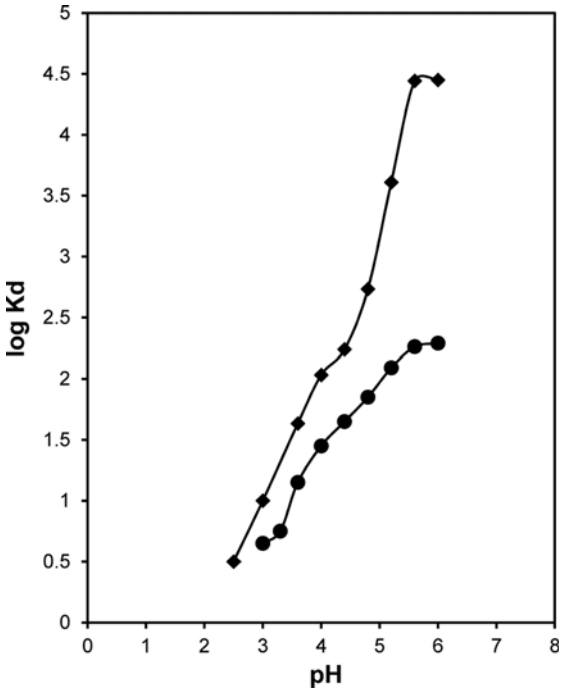


**Fig. 6. Effect of pH on the competitive sorption of strontium ions onto amorphous $MnO_2$-$ZrO_2$ composite (0.2 g) and $MnO_2$-$ZrO_2$ nano-composite (0.05 g). Experimental conditions: initial concentration of the metal ions 50 mg/*l*; volume of aqueous phase 20 and 5 ml for bulk and nano-adsorbents respectively; stirring time 60 min; temperature 25 °C.**

A remarkable enhancement in uptake of Sr(II) ions is presented by means of $MnO_2$-$ZrO_2$ nano-composite. In fact, a shift of the uptake percentage towards lower pH values, and considerable augmentation of removal of strontium ions have resulted by replacing amorphous $MnO_2$-$ZrO_2$ composite by nano-adsorbent. At pH values higher than 5, a quantitative removal of strontium ions was achieved by using nano-adsorbent. Thus pH 5.5 was selected for further experiments.

**3. Effect of Shaking Time**

The adsorption of strontium ions from aqueous solutions adjusted at pH 5.5 on the $MnO_2$-$ZrO_2$ nano-composite (0.05 mg) was studied at different shaking time in the range 5-180 min, and variations of distribution coefficient (log $K_d$) of strontium versus time were plotted (Fig. 7). The results indicate that after 30 min, the absorption kinetics of strontium ions from aqueous solution slowly changes, indicating the distribution coefficient is approximately constant. Therefore, a shaking time of 60 min was selected for the following experiments.

**4. Initial Concentration of Ions**

To investigate the amount of maximum metal ions adsorbed by a given amount of the adsorbent, this variable was tested by the

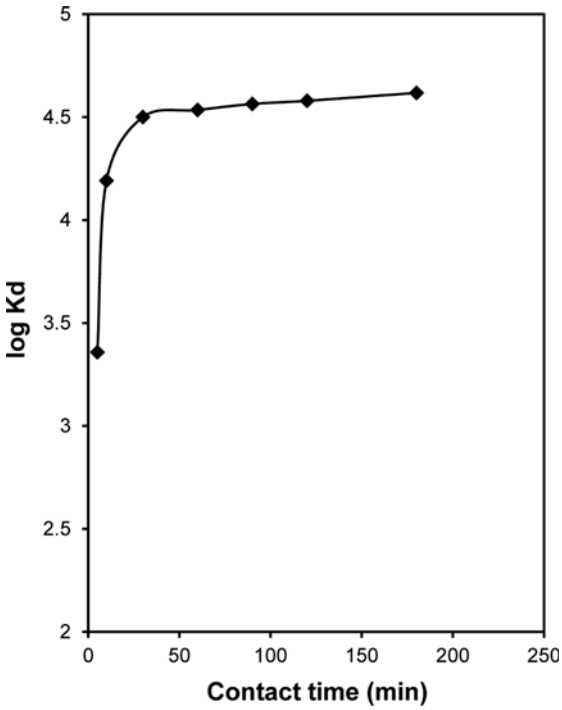


**Fig. 7. Time dependency of the adsorption process of Sr(II) by the $MnO_2$-$ZrO_2$ nano-composite. Aqueous phase pH 5.5, other experimental conditions are as shown in the legend of Fig. 6.**

removal of the studied metal ion with initial concentration in the range 10-500 mg/*l* by 0.05 g of adsorbent at pH 5.5 (Fig. 8). The results show a decrease in the percentage removal of $Sr^{2+}$ ions beyond 50 mg/L of initial concentrations. This observation can be attributed to the relative decrease in the adsorbing sites by increasing the amount of the metal ions.

**5. Adsorption Isotherms**

The adsorption isotherms are mathematical models that describe the relationship between the amount of adsorbate on the adsorbent and the concentration of dissolved adsorbate in the liquid in equilibrium [31]. In this investigation, to evaluate the nature of adsorption, the experimental data were analyzed with the Langmuir, Freundlich and Temkin isotherm models.

The Langmuir sorption isotherm has been widely used to characterize adsorption phenomena from solution. The isotherm is valid for monolayer adsorption onto a surface containing a finite number of identical sites. The form of the Langmuir isotherm can be represented by the following equation [32]:

$$\frac{C_e}{q_e} = \frac{1}{Q^0 b} + \frac{1}{Q^0} C_e \quad (4)$$

where $C_e$ is the equilibrium concentration of ions remaining in the solution (mg/L), and $q_e$ is the amount of metal ions adsorbed per weight unit of the solid after equilibrium (mg/g). The maximum sorption capacity ($Q^0$) is the amount of adsorbate at complete monolayer coverage (mg/g) and b is the constant related to the adsorption intensity (L/mg). The graphic presentations of ($C_e/q_e$) versus $C_e$ give straight lines for $Sr^{2+}$ ions sorbed onto nano-$MnO_2$-$ZrO_2$ (Fig. 9). The numerical values of constants $Q^0$ and b are evaluated from the slope and intercept of plot.

One of the essential characteristics of the Langmuir model could be expressed by a dimensionless constant called equilibrium param-

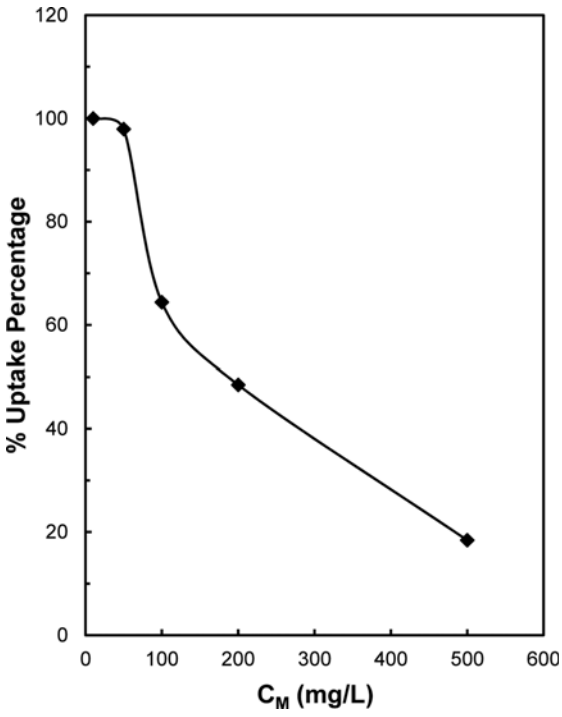


**Fig. 8. Effect of metal ion concentration on the adsorption of strontium ions onto synthesized nano-composite.**

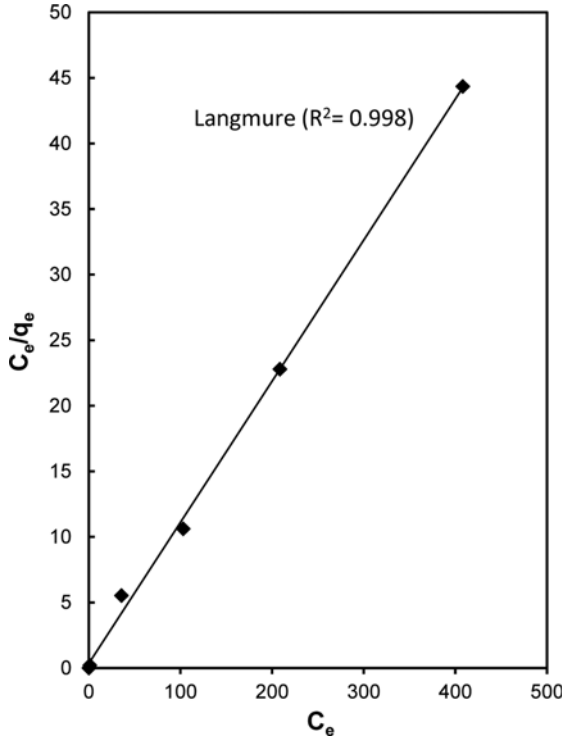


**Fig. 9. Langmuir adsorption isotherm for strontium adsorption on $MnO_2$-$ZrO_2$ nano-composite.**

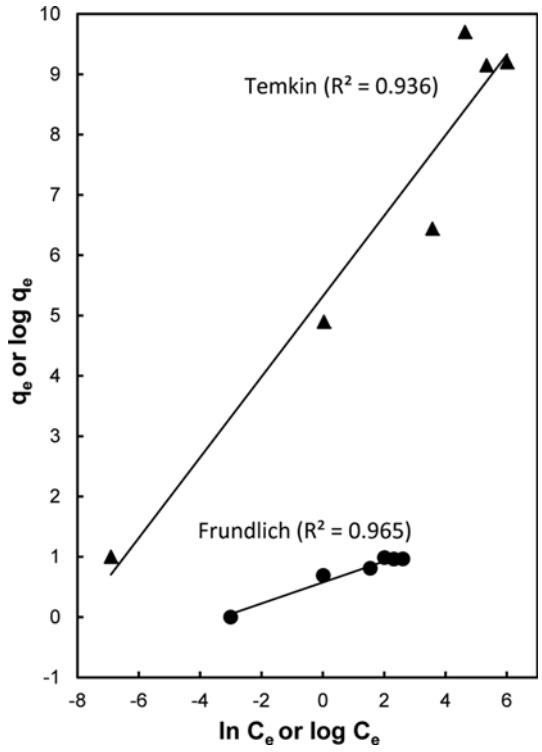


**Fig. 10. Freundlich and Temkin adsorption isotherms for strontium adsorption on $MnO_2$-$ZrO_2$ nano-composite.**

eter $R_L$ [33].

$$R_L = \frac{1}{1+bC_0} \tag{5}$$

$C_0$ is the highest initial metal ion concentration (mg/L). The value of $R_L$ indicates the type of isotherm to be irreversible ($R_L$=0), favorable (0<$R_L$<1), linear ($R_L$=1), or unfavorable ($R_L$>1).

The Freundlich isotherm model stipulates that the ratio of the solute adsorbed to the solute concentration is a function of the solution. This model allows several kinds of sorption sites on the solid and properly represents the sorption data at low and intermediate concentrations on heterogeneous surfaces. The model has the following form [34]:

$$\log q_e = \log K_f + \frac{1}{n}\log C_e \tag{6}$$

where $k_f$ is the constant indicative of the relative ion exchange capacity of the adsorbent (mg/g) and 1/n is the constant indicative of the intensity of the ion exchange/adsorption. A plot of $\log q_e$ versus $\log C_e$ results these constants (Fig. 10). A favorable adsorption condition is created when n>1.

The Temkin equation has the form:

$$q_e = \frac{RT}{b}\ln(aC_e) \tag{7}$$

where R is the gas constant (0.0083 kJ/K·mol) and T is the absolute temperature (K), b is the Temkin constant related to the heat of sorption (kJ/mol), and a is the Temkin isotherm constant (*l*/g). Drawing $q_e$ versus $\ln(C_e)$ allows us to evaluate a, b and the corresponding $R^2$ (Fig. 10).

The parameters calculated from the Langmuir, Freundlich and Temkin isotherm models are summarized in Table 2. The higher correlation coefficients indicate that the Langmuir model fits the adsorption data better than the other models within the entire range of adsorptive concentration studied (Fig. 9). In addition, the evaluated $R_L$ (0.07), in the Langmuir model, confirms the favorable uptake of strontium ions by the examined sorbent.

**6. Kinetics of the Adsorption Processes**

The rate of extraction of strontium ions by $MnO_2$-$ZrO_2$ nanocomposite was studied by equilibrating the 0.05 g solid phase with a series of ion solutions for different time intervals. Fig. 7 shows the amount of strontium adsorbed at a contact time, t (min). To investigate the specific rate constant of the present adsorption reactions, the kinetic data were analyzed by the reversible first-order and pseudo-second order kinetic model equations. The mathematical linear form of the equations used and the plots developed for analyzing the data are given in Table 3.

The pseudo-first-order model equation is written in Eq. (8):

$$\log(q_e - q_t) = \log q_e - \frac{k_1}{2.303}t \tag{8}$$

where $q_e$ and $q_t$ are the amounts of metals adsorbed on the sorbent (mg/gr) at equilibrium and at time t, respectively, and $k_1$ is the rate constant of the first-order adsorption ($min^{-1}$). The straight line plots of log ($q_e$–$q_t$) against t were used to determine the rate constant, $k_1$ and correlation coefficient, $R^2$ values of the metals were calculated from this plot (Fig. 11). The calculated correlation coefficient for pseudo-first-order and the values of constants are shown in Table 3.

A mathematical expression of the pseudo-second-order model

**Table 2. Sorption isotherm parameters for strontium ions onto $MnO_2$-$ZrO_2$ nano composite**

| Metal ion | Langmuir model | | | | Freundlich model | | | Temkin model | | |
|---|---|---|---|---|---|---|---|---|---|---|
| | $R^2$ | $R_L$ | $Q_0$ (mg/g) | b (L/mg) | $R^2$ | $K_f$ (mg/g) | n | $R^2$ | a (L/g) | b (kJ/mol) |
| Sr(II) | 0.998 | 0.007 | 9.346 | 0.300 | 0.965 | 3.750 | 5.743 | 0.936 | 4.195 | 3.708 |

**Table 3. Pseudo first and second order kinetic models parameters for strontium ion**

| | Pseudo-first-order | | | Pseudo-second-order | | | |
|---|---|---|---|---|---|---|---|
| | $q_e$ (mg/g) | $K_1$ ($min^{-1}$) | $R^2$ | $q_e$ (mg/g) | $K_2$ (mg/g·min) | $h_0$ (mg/min) | $R^2$ |
| Sr(II) | 3.020 | $2.303\times10^{-5}$ | 0.461 | 5.000 | 2.105 | 52.632 | 1.000 |

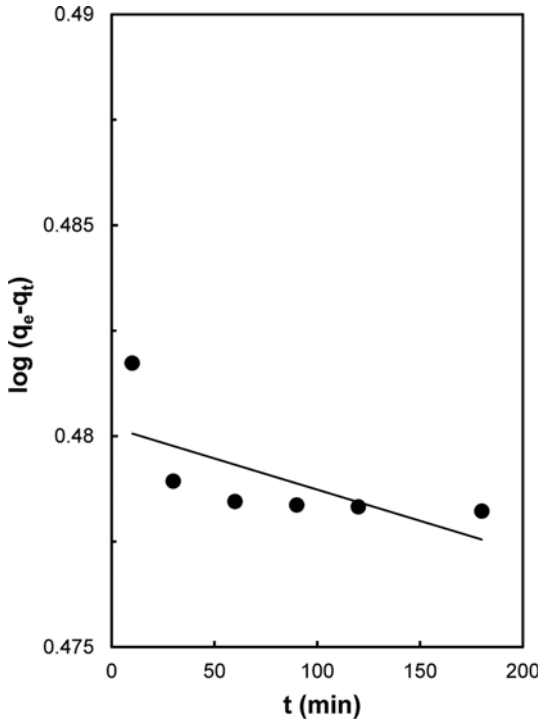


**Fig. 11. The pseudo-first-order kinetic plot of strontium adsorption on $MnO_2$-$ZrO_2$ nano-composite.**

is shown in Eq. (9):

$$\frac{t}{q_t}=\frac{1}{k_2 q_e^2}+\frac{t}{q_e} \quad (9)$$

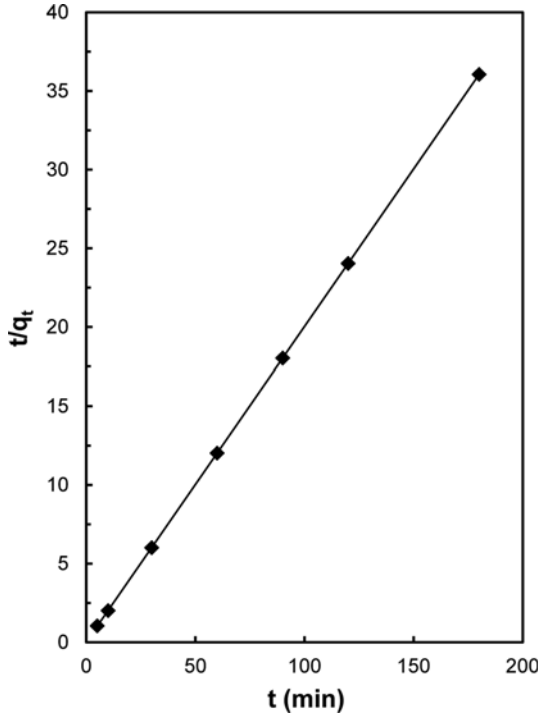


**Fig. 12. The pseudo-second-order kinetic plot of strontium adsorption on $MnO_2$-$ZrO_2$ nano-composite.**

where t is time (min), $q_t$ and $q_e$ are the quantity of adsorbed ions on the surface of sorbent (mg/g) at time t and at equilibrium, respectively, and $k_2$ denotes the pseudo-second-order rate constant (g/mg·min). The values of constants and correlation coefficients for pseudo-second-order can be calculated from the slope and intercept of plot of $t/q_t$ versus t (Fig. 12).

In this model the initial rate of sorption can be evaluated as $q_t/t$ approaches to zero, it means:

$$h_0=k_2 q_e^2 \quad (10)$$

where $h_0$ is the initial rate of sorption (mg/g·min).

The results obtained from the analysis of the present data indicated that strontium adsorptions on $MnO_2$-$ZrO_2$ nano-composite best described ($R^2$=1.00) by pseudo-second order kinetic equation.

**7. Adsorption Studies**

To determine the potential ability of the $MnO_2$-$ZrO_2$ nano-composite in the separation of metal ions, distribution coefficient ($K_d$) studies for various metal ions under the optimized conditions were conducted. The results are listed in Table 4. The distribution coefficients of the metal ions on this adsorbent showed a great affinity of this material for a number of ions such as Sr(II), Y(III), Ni(II), Pb(II) and Co(II) in water. The selectivity coefficients of Sr(II), Y(III), Ni(II), Pb(II) and Co(II) ions in other inorganic cations were studied by batch procedure. The selectivity of the Sr(II), Y(III), Ni(II), Pb(II) and Co(II) ions versus another cation was determined by the ratio of the two distribution coefficients, $K_d$Sr(II), Y(III), Ni(II), Pb(II) and Co(II) and $K_d$M(n), which is referred to as the selectivity factor (Eq. (11)):

$$\alpha = K_d\text{Sr(II), Y(III), Ni(II), Pb(II), Co(II)}/K_d\text{M(n)} \quad (11)$$

**Table 4. Distribution coefficients of metal ions on of nano-structured $MnO_2$-$ZrO_2$**

| Metal ions | $K_d$ values (ml/g) |
|---|---|
| Sr (II) | T. A* |
| Zr (IV) | 534 |
| Mo (VI) | 218 |
| Pb (II) | 9347 |
| Co (II) | 7156 |
| Y (III) | T. A* |
| Hg (II) | 1777 |
| Ni (II) | T. A* |
| La (III) | 17.8 |

*Total adsorption

**Table 5. Selectivity coefficients of Sr(II), Y(III), Ni(II), Pb(II) and Co(II) ions over other inorganic cations**

| Metal ions | Selectivity factor ($\alpha$) | | |
|---|---|---|---|
| | for Co (II) | for Pb (II) | for Sr (II), Ni (II), Y (III) |
| Zr (IV) | 13.40 | 17.50 | >1000 |
| Mo (VI) | 32.82 | 42.88 | >1000 |
| Hg (II) | 4.03 | 5.26 | >100 |
| La (III) | 402.02 | 525.11 | $>10^5$ |

The obtained results are summarized in Table 5. It is clear from the results that the quantitative separation of strontium ions from Zr(IV), Mo(VI) and La(III) are possible.

## CONCLUSION

A supercritical water impregnation method in the hydrothermal crystallization process for the synthesis of $MnO_2$-$ZrO_2$ nano-composite is reported. It was characterized with chemical and physical methods. This composite showed high ion-exchange ability towards strontium ions in comparison with $MnO_2$-$ZrO_2$ non-nano adsorbent. It also showed a strong affinity toward the Y(III), Ni(II), Pb(II) and Co(II). Therefore, the synthesized nano-composite could be used to remove and separate these heavy toxic metals from the nuclear radioactive waste. The results are promising and would be useful for synthesizing other types of similar composites for the waste treatment purpose.

## REFERENCES


1. M. Hua, Sh. Zhang, B. Pan, W. Zhang, L. Lv and Q. Zhang, *J. Hazard. Mater.*, **211-212**, 317 (2012).
2. C. Karthika and M. Sekar, *I Res. J. Environ. Sci.*, **1**, 34 (2012).
3. C. N. R. Rao and A. K. Cheetham, *J. Mater. Chem.*, **11**, 2887 (2001).
4. H. Badaruddin Ahmad, Y. Abbas, M. Hussain, N. Akhtar, T. Ansari, M. Zuber, Kh. Mahmood Zia and Sh. Ahmad Arain, *Korean J. Chem. Eng.*, **31**, 284 (2014).
5. A. Ramazanpour Esfahani, S. Hojati, A. Azimi, L. Alidokht, A. Khataee and M. Farzadian, *Korean J. Chem. Eng.*, **31**, 630 (2014).
6. H. I. Adegoke, F. A. Adekola, O. S. Fatoki and B. J. Ximba, *Korean J. Chem. Eng.*, **31**, 142 (2014).
7. Z. Shiri-Yekta, M. R. Yaftian and A. Nilchi, *Korean J. Chem. Eng.*, **30**, 1644 (2013).
8. T. Adschiri, K. Kanazawa and K. Arai, *J. Am. Ceram. Soc.*, **75**, 1019 (1992).
9. T. Adschiri, K. Kanazawa and K. Arai, *J. Am. Ceram. Soc.*, **75**, 2615 (1992).
10. Y. Hakuta, T. Adschiri, T. Suzuki, T. Chida, K. Seino and K. Arai, *J. Am. Ceram. Soc.*, **81**, 2461 (1998).
11. Y. Hakuta, T. Adschiri, H. Hirakoso and K. Arai, *Fluid Phase Equilib.*, **158-160**, 733 (1999).
12. T. Adschiri, Y. Hakuta and K. Arai, *J. Ind. Eng. Chem. Res.*, **39**, 4901 (2000).
13. K. Kanamura, A. Goto, R. Ho, T. Umegaki, K. Toyoshima, K. Okada, Y. Hakuta, T.Adschiri and K. Arai, *J. Electrochem. Solid-State Lett.*, **3**, 256 (2000).
14. Y. Hakuta, K. Seino, H. Ura, T. Adschiri, H. Takizawa and K. Arai, *J. Mater. Chem.*, **9**, 2671 (1999).
15. A. Cabanas, J. A. Darr, E. Lester and M. Poliakoff, *J. Chem. Commun.*, **11**, 901 (2000).
16. A. Cabanas, J. A. Darr, E. Lester and M. Poliakoff, *J. Mater. Chem.*, **11**, 561 (2001).
17. S. J. Ahmadi, N. Akbari, Z. Shiri-Yekta, M. H. Mashhadizadeh and A. Pourmatin, *J. Radioanal. Nucl. Chem.*, DOI:10.1007/s10967-013-2852-9.
18. J. K. Moon, K. W. Kim, C. H. Jung, Y. G. Shul and E. H. Lee, *J. Radioanal. Nucl. Chem.*, **246**, 299 (2000).
19. A. Nilchi, A. Khanchi, H. Atashi, A. Bagheri and L. Nematollahi, *J. Hazard. Mater.*, **A137**, 1271 (2006).
20. A. R. Khanchi, R. Yavari and S. K. Pourazarsa, *J. Radioanal. Nucl. Chem.*, **273**, 141 (2007).
21. A. Nilchi, M. R. Hadjmohammadi, S. Rasouli Garmarodi and R. Saberi, *J. Hazard. Mater.*, **167**, 531 (2009).
22. S. J. Ahmadi, S. Sadjadi and M. Hosseinpour, *J. Ultrason. Sonochem.*, **20**, 408 (2013).
23. M. Outokesh, M. Hosseinpour, S. J. Ahmadi, T. Mousavand, S. Sadjadi and W. Soltanian, *J. Ind. Eng. Chem. Res.*, **50**, 3540 (2011).
24. I. M. Ali, A. A. El-Zahhar and E. S. Zakaria, *J. Radioanal. Nucl. Chem.*, **264**, 637 (2005).
25. S. H. El-Khouly, *J. Radioanal. Nucl. Chem.*, **270**, 391 (2006).
26. E. Metwally, T. El-Zakla and R. R. Ayoub, *J. Nucl. Radiochem. Sci.*, **9**, 1 (2008).
27. M. Davis, Elsevier Publishing Co., Amsterdam, 318 (1963).
28. S. P. Mishra, S. S. Dubey and D. Tiwari, *J. Radioanal. Nucl. Chem.*, **261**, 457 (2004).
29. V. Vesely and V. Pekarek, *Talanta*, **19**, 219 (1972).
30. S. Inan, H. Tel and Y. Altas, *J. Radioanal. Nucl. Chem.*, **267**, 615 (2006).
31. J. Peric, M. Trgo and N. V. Medvidovic, *J. Water Res.*, **38**, 1839 (2004).
32. I. Langmuir, *J. Am. Chem. Soc.*, **40**, 1361 (1918).
33. D. Mohan and S. Chander, *J. Colloid Interface Sci.*, **299**, 57 (2006).
34. H. Freundlich, *Z. Phys. Chem.*, **57**, 384 (1906).